JOURNAL OF SPACECRAFT AND ROCKETS
Vol. 37, No. 5, September–October 2000

Thermally Induced Dynamics of Satellite Solar Panels

John D. Johnston* and Earl A. Thornton†
University of Virginia, Charlottesville, Virginia 22903

Thermally induced structural motions are known to affect the attitude dynamics of low Earth orbiting satellites during eclipse transitions. Motions of flexible appendages such as solar panels lead to rigid body rotations of the entire satellite because the total angular momentum of the system is conserved. These potentially large attitude disturbances may violate pointing accuracy and jitter requirements. One type of thermally induced dynamics exhibited by solar panels is thermal snap. The Upper Atmosphere Research Satellite is a prominent example of a satellite that experiences thermal snap disturbances during eclipse transitions. This paper describes recent studies of thermally induced dynamics of solar panels, including an analysis of satellite attitude dynamics resulting from thermally induced structural motions and a laboratory investigation of the thermal-structural performance of a satellite solar panel. Analytical and experimental results demonstrate thermal bending deformations with acceleration transients that have characteristic thermal snap disturbance histories in response to rapid changes in heating. The studies show that solar panel thermal snap disturbances are caused by through-the-thickness temperature differences that vary at a nonconstant rate. Finite element analysis correctly predicts the thermal snap phenomenon observed in the solar panel experiments.

Nomenclature

A	=	cross-sectional area, m^2
c	=	specific heat, J/kg · K
c_{damp}	=	damping constant, kg/m · s
h	=	facesheet centroid separation distance, m
I_{sat}	=	composite mass moment of inertia for satellite, kg · m^2
k	=	thermal conductivity, W/m · K
L	=	length, m
M_T	=	thermal moment, N · m
q	=	generalized modal coordinate
R_0	=	hub radius, m
S	=	solar heat flux, W/m^2
T	=	temperature, K
T_{ref}	=	reference temperature, K
T_{TID}	=	thermally induced disturbance torque, N · m
t	=	time, s
v	=	displacement, m
v_{qs}	=	quasi-static displacement, m
W	=	width, m
x, y, z	=	spatial coordinates, m
α_{cte}	=	coefficient of thermal expansion, 1/K
ΔT	=	temperature difference, K
ζ	=	damping coefficient
θ	=	attitude angle, rad
θ_{qs}	=	quasi-static attitude angle, rad
ν	=	Poisson's ratio
ρ	=	density, kg/m^3
ϕ	=	shape function
ω	=	natural frequency, rad/s

Introduction

THE thermal-structural performance of deployable appendages can have a significant effect on the attitude dynamics and control of satellites. Nonuniform thermal loading may give rise to cross-sectional temperature differences in appendages which, due to differential thermal expansion, result in thermoelastic deformations. Additionally, rapid changes in thermal loading initiated as a satellite exits or enters the Earth's shadow can excite dynamic structural motions. Thermally induced structural motions (TISMs) of flexible satellite appendages may be classified as thermal bending, thermal snap, thermally induced vibrations, or thermal flutter.[1–3] Thermal bending motions are quasi-static structural deformations that result from slowly varying temperature differences. A quasi-static deformation consists of a succession of equilibrium displacements each corresponding to the temperature difference at a given instant in time. Since the temperature differences driving thermal bending motions develop slowly, appendage accelerations are very small. Thermal snap (or thermoelastic shock) motions involve rapid, nonoscillatory appendage deformations that are initiated during orbital eclipse transitions. A thermal snap response is similar to quasi-static TISMs in that it consists of a succession of quasi-equilibrium displacements that result from time-varying temperature differences in appendages. However, in the thermal snap case, the rapid rise and decay of the temperature differences result in short duration acceleration transients at times corresponding to eclipse transitions. Thermally induced vibrations, which consist of a quasi-static deformation with superimposed oscillations, are a stable dynamic response and may involve bending (flexural), torsional, or combined bending and torsional motions. Similar to thermal snap disturbances, thermally induced vibrations typically occur when flexible appendages are subjected to rapidly developing or decaying temperature differences such as when the satellite undergoes an eclipse transition. The most severe type of TISM is thermal flutter. Thermal flutter is an unstable thermally induced vibrations response. The instability mechanism is coupling between incident heating and structural deformations. In the cases described previously, the structural motions involve thermoelastic bending deformations driven by time-varying temperature differences. Structural dynamics may also be initiated by thermally induced stick-slip motions in mechanisms, a phenomenon generally referred to as thermal creak.[4]

A common solar array design is the rigid panel solar array, which is made up of one or more solar panels. Each panel consists of a honeycomb sandwich panel substrate onto which solar cells are mounted. Mathematical modeling of satellite attitude disturbances resulting from TISMs of solar panels has been investigated by several authors. Bainum et al.[5] studied thermal bending of free-free beams and plates subject to sudden changes in thermal loading to predict the effect on satellite attitude dynamics and control. Zimbelman[6] and Zimbelman et al.[7] performed an analysis of the disturbance affecting the TOPEX satellite and developed an analytical model for predicting the disturbance torques resulting from thermally induced deformations of rigid panel solar arrays initiated

Received 21 January 2000; revision received 25 April 2000; accepted for publication 29 April 2000.

*Graduate Research Assistant, Department of Mechanical and Aerospace Engineering; currently Aerospace Engineer, NASA Goddard Space Flight Center, Greenbelt, MD 20771. Member AIAA.

†Professor Emeritus, Department of Mechanical and Aerospace Engineering. Fellow AIAA.

during eclipse transitions. These studies utilized a quasi-static approach for formulating the solar array structural response and the corresponding thermal snap disturbance torque. Recently, Johnston and Thornton[8,9] studied the coupled dynamics of a simple satellite with a solar panel that experiences TISMs. The study utilized a formulation that includes both quasi-static and dynamic terms in calculating the solar panel response. Several aspects of the solar panel thermal snap problem have unanswered questions. First, what is the explanation for the observed characteristics of satellite motions resulting from thermal snap disturbances? Second, how do they differ from a thermally induced vibrations response? Additionally, there is a lack of experimental data for thermally induced dynamics for use in validating analytical models and investigating the performance of satellite hardware. Thus, further research is needed to improve analytical models for predicting thermally induced solar panel dynamics and to characterize the thermal snap of solar panels experimentally.

The overall objective of the present paper is to provide a detailed explanation of solar panel thermal snap disturbances. First, a review of flight data that demonstrates the thermal snap disturbance affecting the Upper Atmosphere Research Satellite (UARS) is presented. Then, two recent studies[2] carried out to investigate solar panel thermal snap are described. The first study utilizes an analytical formulation for the coupled dynamics of a simple satellite with a solar panel to study the effects of thermal snap disturbances on satellite attitude dynamics. The second study investigates the thermal-structural performance of a satellite solar panel experimentally. The experimental study utilizes a solar panel assembly from the NASA Transition Region and Coronal Explorer (TRACE) satellite to characterize the thermal-structural response of satellite solar array hardware to laboratory-simulated orbital eclipse transition heating. Results from the experiments are used to validate finite element models for solar panel thermal-structural behavior.

UARS Thermal Snap

The UARS satellite experiences attitude disturbances during orbital eclipse transitions due to rapid thermal bending of its rigid panel solar array. The disturbances are of sufficient magnitude to violate the stability requirements for some of the science instruments on the satellite. Figure 1a presents a schematic of the UARS satellite, which utilizes a single wing rigid panel solar array. Flight data[10] demonstrating the attitude acceleration (roll, pitch, and yaw shown in arcsec/s^2) during a sunrise orbital eclipse transition are presented in Fig. 1b. The satellite attitude was calculated from fixed-head star trackers and inertial reference unit data, and postprocessed to determine the attitude accelerations. The disturbance is manifested predominately in the roll (X) and yaw (Z) responses. The first peak in the roll response is approximately -1.8 arcsec/s^2, followed by another peak of $+1.5$ arcsec/s^2. Note that the form of the acceleration transient resembles a impulselike negative spike followed by a positive steplike response that exponentially decays to zero. The entire disturbance transient lasts approximately 100 s. This behavior is representative of a typical thermal snap disturbance torque that consists of a short duration transient having two parts: an impulselike response followed by exponentially decaying steplike response of the opposite sign.[6] In the following sections, the results of analytical and experimental studies of solar panel thermal-structural behavior are used to explain the characteristics of the thermal snap disturbances observed in satellite flight data.

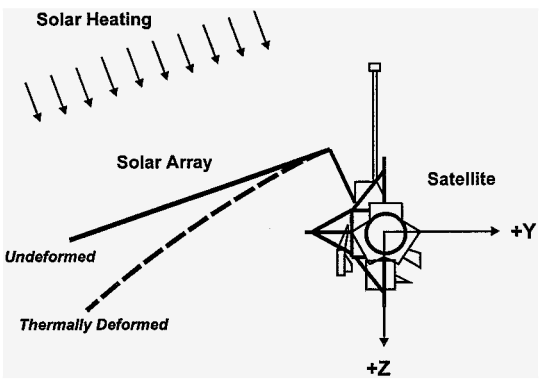

a) Schematic of UARS satellite and solar array

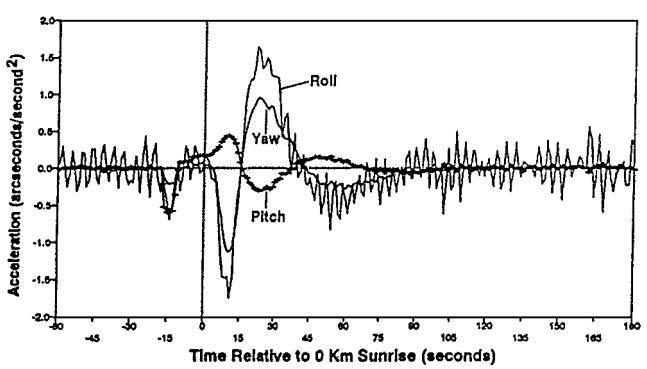

b) Attitude acceleration response for sunrise orbital eclipse transition[10]

Fig. 1 UARS satellite thermal snap disturbance.

Analytical Studies

This section presents an analysis of the problem of TISMs of solar panels initiated during eclipse transitions and their effect on satellite attitude dynamics. The objectives of the analyses are to predict the thermal response of solar panels to orbital eclipse transition heating and to predict the dynamics of a simple satellite with a solar panel undergoing TISMs. First, the solar panel thermal analysis is presented, followed by the satellite dynamics analysis. Then, a numerical example is given to demonstrate the thermal and dynamic responses of a simple satellite during a sunrise eclipse transition.

Thermal Analysis

The thermal analysis involves two steps: 1) calculation of the incident heating and 2) calculation of the solar panel thermal response.

Orbital Eclipse Heating

The orbital eclipse heating analysis calculates the time-varying heating experienced by a satellite during orbital eclipse transitions. Consider the case of a sunrise eclipse transition. Initially, the satellite is in the region of total shadow called the umbra. The satellite then crosses through the region of partial shadow (penumbra) and finally emerges into full sunlight. The intensity of the incident solar heat flux experienced by a satellite in the penumbra is proportional to the area of the solar disk that is visible to the satellite. This area is determined by considering the angular sizes of the Earth/sun disks and the angular separation between the centers of the Earth and sun as viewed from the satellite. The time history of the incident heating must be determined accurately to predict the solar panel thermal response. The heating analysis makes the following assumptions: 1) the satellite is in a circular orbit, 2) the orbit plane coincides with the plane of the Earth's orbit around the sun (the ecliptic plane), and 3) variations in solar heating dominate the thermal response during eclipse transitions; thus, Earth-reflected (albedo) and Earth-emitted heat fluxes are neglected. The orbital eclipse heating analysis calculates the actual solar heat flux history during penumbral transition based on the geometry of the sun-Earth-satellite system utilizing results given by Baker.[11]

Solar Panel Thermal Response

The thermal response of the solar panel subject to the calculated time-varying incident heating was determined using finite element analysis. The results of the thermal analysis are required for input to solar panel thermal-structural models in the satellite dynamics analysis. Traditional thermal analyses for satellite structures are performed to predict surface temperature histories. For TISMs studies, it is necessary to also calculate cross-sectional temperature difference histories as well as the first and second time derivatives of the temperature difference as functions of time.

The thermal analysis assumes one-dimensional conduction through the thickness of the solar panel subject to radiation boundary conditions on the front and back surfaces. The boundary conditions

consist of a uniform solar heat flux $S(t)$ directed normal to the front surface of the solar panel and thermal radiation from the front and back surfaces to a deep space temperature of 0 K. The solar heat flux $S(t)$ is calculated as described in the previous section. The analysis assumes that the solar panel is sun-tracking over the entire orbit, thus the solar heat flux is always incident normal to the front surface of the panel. Also, the absorbed heat flux is assumed to remain constant for small solar panel deformations, that is, the thermal response is assumed to be independent of the structural response. The temperature of the solar panel, $T(z, t)$, is assumed to be uniform in the x and y directions and to vary through the thickness of the panel in the z direction. The temperatures at the surfaces of the front and back facesheets are $T_{\text{front}}(t)$ and $T_{\text{back}}(t)$, respectively. The temperature difference through the thickness of the solar panel is given by $\Delta T(t) = T_{\text{front}}(t) - T_{\text{back}}(t)$. The transient thermal response was computed using the commercial finite element analysis program ABAQUS.[12] The one-dimensional finite element model of the solar panel uses a total of 25 two-node rod elements through the thickness of the panel. Each of the different layers in the solar panel (facesheets, adhesive, and core) is represented in the model. The honeycomb core is represented as a solid using effective properties. Postprocessing yields the temperature difference through the thickness of the panel and the time derivatives of the temperature difference that are required for solar panel structural response studies. Studies performed using a three-dimensional model demonstrated that the one-dimensional model is accurate for the case of uniform heating of an solar panel with isotropic in-plane properties, that is, where in-plane heat transfer is negligible. The topic of solar panel thermal modeling will be revisited later in the paper during the discussion of the analysis of the laboratory experiments.

Satellite Dynamics Analysis

The objective of the satellite dynamics analysis is to investigate the effects of TISMs on the planar dynamics of a simple satellite that consists of a rigid hub and a flexible solar panel. The approach taken is based on a technique developed by Junkins and Kim[13] that utilizes a generalized form of Lagrange's equations to obtain the governing equations of motion and boundary conditions for a class of hybrid coordinate multibody systems representative of satellites with flexible appendages. Using this approach, a new formulation for the problem of TISMs was presented by Johnston and Thornton[8] and is used herein.

The problem considered is the planar motions of a simple satellite, Fig. 2, consisting of a rigid hub and a cantilevered flexible solar panel. The rigid hub has a mass m_{hub} and a radius R_0. The flexible solar panel is modeled as a beam of length L, mass per unit length ρA, and bending stiffness EI. The two coordinate systems used in the analysis are also shown in Fig. 2. The I1–I2 axes are located in an inertial reference frame fixed with respect to motions of the satellite. The B1–B2 axes are located in a body fixed reference frame

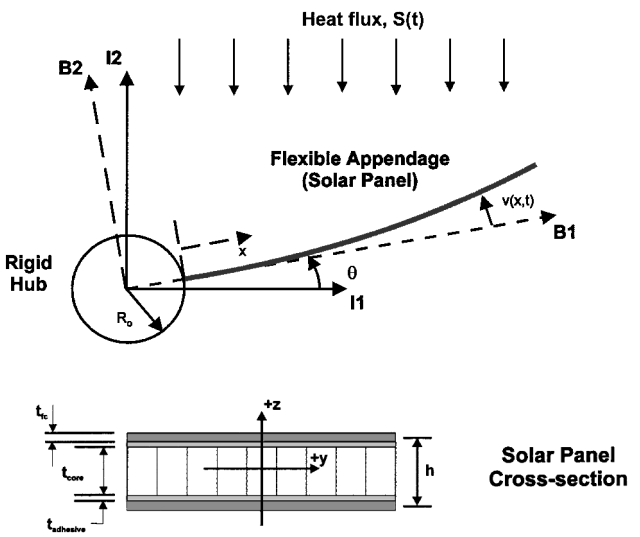

Fig. 2 Satellite mathematical model and coordinate systems.

attached to the hub with the B1 axis coinciding with the neutral surface of the undeformed solar panel. The origins of both sets of axes coincide with the center of the hub. The attitude angle $\theta(t)$ measures rigid body rotations of the hub about its center, and $v(x, t)$ is the displacement of the flexible appendage relative to the B1 axis. Only planar motions of the system consisting of small rotations of the hub about its center and bending motions of the solar panel in the I1–I2 plane are considered. There are no external forces or moments acting on the system, so the total angular momentum is conserved.

The governing equations for the coupled dynamic response of the system are obtained using a generalized form of Lagrange's equations for hybrid coordinate systems. The resulting governing equation for the rigid body rotations of the hub is given by

$$I_{\text{sat}}\ddot{\theta} + \int_0^L \rho A(R_0 + x)\ddot{v}(x, t)\,\mathrm{d}x = 0 \tag{1}$$

An expression for the thermally induced disturbance torque $T_{\text{TID}}(t)$ is obtained from Eq. (1) by moving the terms corresponding to motions of the flexible solar panel to the right-hand side of the equation:

$$T_{\text{TID}}(t) = -\rho A \int_0^L (R_0 + x)\ddot{v}(x, t)\,\mathrm{d}x \tag{2}$$

Note that the thermally induced disturbance torque is directly proportional to the second time derivative of the solar panel displacements. The governing equation for the solar panel deformations in the body fixed reference frame is given by

$$\rho A(R_0 + x)\ddot{\theta} + \rho A\ddot{v} + c_{\text{damp}}\dot{v} + EIv^{\text{IV}} = 0 \tag{3}$$

where $c_{\text{damp}} = 2\zeta\omega_n\rho A$ is an equivalent viscous damping constant representing structural damping, ω_n are the natural frequencies of the solar panel, and ζ is the damping factor. The boundary conditions for the solar panel are

$$v(0, t) = 0 \tag{4a}$$

$$v'(0, t) = 0 \tag{4b}$$

$$EIv''(L, t) + M_T(t) = 0 \tag{4c}$$

$$EIv'''(L, t) = 0 \tag{4d}$$

where at $x = 0$ the solar panel is fixed and at $x = L$ the solar panel is free. Note that in Eq. (4c), the usual boundary condition of zero moment at a free end is modified by the inclusion of the thermal bending moment $M_T(t)$. The development of the following expression for the thermal moment in a solar panel is given in Ref. 2:

$$M_T(t) = E_{\text{fc}}\alpha_{\text{cte}}\,(Wt_{\text{fc}}h/2)\,\Delta T(t) \tag{5}$$

where E_{fc} is the modulus of elasticity for the facesheets, α_{cte} is the coefficient of thermal expansion of the facesheets, W is the width of the solar panel, t_{fc} is the facesheet thickness, h is the separation distance between the facesheets, and $\Delta T(t)$ is the through-the-thickness temperature difference. The time-dependent thermal moment acts as the forcing term in the solar panel equations of motion.

Quasi-Static Response

A quasi-static response occurs for the case where inertia effects are negligible, that is, when there are negligible vibrations. The quasi-static structural response consists of a succession of equilibrium displacements that correspond to the temperature distribution at a given instant in time. The quasi-static displacements of the solar panel, $v_{\text{qs}}(x, t)$, are obtained by neglecting terms corresponding to inertia forces in Eq. (3). Solving Eq. (3) subject to the boundary conditions Eq. (4) yields the following solution for the quasi-static displacements:

$$v_{\text{qs}}(x, t) = \frac{-M_T(t)}{2EI}x^2 \tag{6a}$$

A modified bending stiffness $EI = E_{fc}t_{fc}h^2W/[2(1-\nu^2)]$ is utilized to account for the structure being a relatively wide as opposed to a narrow-width beam. The quasi-static displacements can be expressed in terms of the temperature difference through the thickness of the solar panel by substituting Eq. (5) for the thermal moment into Eq. (6a), giving

$$v_{qs}(x,t) = \left[-\alpha_{cte}(1-\nu^2)\Delta T(t)/2h\right]x^2 \tag{6b}$$

This result shows that, for a positive value of $\Delta T(T_{front} > T_{back})$, the solar panel will exhibit negative displacements, that is, bend away from the direction of the incident heating. The displacements vary spatially with the square of the distance x along the solar panel and vary in time due to the time dependence of the through-the-thickness temperature difference. Differentiating Eq. (6b) with respect to time yields the velocity and acceleration of the solar panel that are directly proportional to the first and second time derivatives of the through-the-thickness temperature difference. These derivatives are normally zero except for a short interval of time surrounding eclipse transitions when the temperature difference varies at a nonconstant rate.

Dynamic Response

An approximate form of the equations of motion stated in Eqs. (1) and (3) is obtained using the quasi-static solution and modal expansion. The assumed form of the solution is

$$v(x,t) = v_{qs}(x,t) + \sum_{n=1}^{N} \phi_n(x)q_n(t) \tag{7}$$

where $v_{qs}(x,t)$ is the quasi-static response, $\phi_n(x)$ are the nth shape functions, $q_n(t)$ are the nth generalized modal coordinates, and N is the number of modes considered. The shape functions are chosen to be the eigenfunctions from the free vibration response of a fixed-base cantilevered beam. Substituting the assumed form of the displacements into the governing equations, a system of $N+1$ coupled linear ordinary differential equations for the discrete coordinate $\theta(t)$ and the generalized modal coordinates $q_n(t)$ is obtained. The resulting equations are written in matrix form as

$$[M]\{\ddot{x}\} + [C]\{\dot{x}\} + [K]\{x\} = \{F(t)\} \tag{8}$$

where $\{x\}^T = \{\theta \;\; q_1 \;\; q_2 \;\; \cdots \;\; q_N\}$ are the generalized coordinates for the system and $[M]$, $[C]$, and $[K]$ are $N+1$ by $N+1$ constant coefficient matrices. The forcing vector $\{F(t)\}$ contains terms involving time derivatives of the temperature difference through the thickness of the solar panel. Thus, both the temperature difference and its time derivatives are key parameters in the study of TISMs. Numerical integration of the governing equations leads to solutions for the thermally induced dynamics of the satellite.

Disturbance Torque

Recall that during eclipse transitions a disturbance torque arises due to the acceleration of the solar panel. Substituting Eq. (7) into Eq. (2) results in a new expression for the thermally induced disturbance torque $T_{TID}(t)$, which consists of a superposition of quasi-static $T_{QS}(t)$ and vibratory $T_{VIBE}(t)$ terms:

$$T_{TID}(t) = -[T_{QS}(t) + T_{VIBE}(t)] \tag{9}$$

where

$$T_{QS}(t) = \left[\rho A\alpha_{cte}(1-\nu^2)\big/2h\right]\left(R_0L^3/3 + L^4/4\right)\Delta\ddot{T} \tag{10a}$$

$$T_{VIBE}(t) = \rho A\sum_{n=1}^{N}\left[\int_0^L (R_0+x)\phi_n(x)\,dx\right]\ddot{q}_n(t) \tag{10b}$$

The quasi-static component of the thermally induced disturbance torque, Eq. (10a), is directly proportional to the second time derivative of the temperature difference through the thickness of the solar panel, whereas the vibratory component, Eq. (10b), is proportional to the second time derivatives of the modal amplitudes. The relative dominance of the quasi-static and vibratory terms determines the type of response exhibited by the system. Systems for which the quasi-static term dominates experience thermal snap disturbances, whereas systems in which the vibratory term dominates exhibit thermally induced vibrations.[2]

Table 1 Solar panel parameters for thermal response numerical examples

Parameter	Facesheet	Adhesive	Honeycomb core
Material	Aluminum 6061	Epoxy	Aluminum 5056
Thickness, m	2.54E−04	1.27E−04	0.0254
Thermal conductivity, W/m · K	168	0.4	1.2
Density, kg/m^3	2800	1150	30.0
Specific heat, J/Kg · K	960	750	920

Numerical Example

The following numerical example illustrates the thermal snap phenomenon for a simple satellite with a solar panel undergoing TISMs. Results for the thermal response of the solar panel and the dynamic motions of the satellite are presented.

Thermal Response

Finite element analysis was used to predict the thermal response of a solar panel subject to orbital eclipse transition heating. The analysis considers the case of a 600 km circular orbit whose orbital plane lies in the ecliptic. This altitude is representative of typical low Earth orbital satellite altitudes, such as that used by the UARS satellite. The parameters used in the study are given in Table 1 and are representative of typical satellite solar panels. Additionally, the front surface of the solar panel has an absorptivity $\alpha = 0.79$ and an emissivity $\varepsilon = 0.81$, whereas the back surface has an emissivity $\varepsilon = 0.86$.

The incident solar heating and solar panel thermal response during a sunrise orbital eclipse transition are presented in Fig. 3. The incident solar heat flux history is given in Fig. 3a. At $t = 0$, the solar panel is in total shadow ($S = 0$ W/m^2), and at $t = 10$ s, it enters the penumbra and begins the transition to full sunlight ($S = 1350$ W/m^2). The transition time between total shadow and full sunlight is approximately 8.5 s. Figures 3b and 3c present plots of the surface temperatures and temperature difference as functions of time. Subsequent to entering the penumbra, the surface temperatures begin a gradual rise. However, a temperature difference develops rapidly, reaching its steady-state value of 11 K in approximately 75 s. As noted earlier, the time derivatives of the temperature difference are needed for TISMs studies. Plots of the first and second time derivatives of the temperature difference are given in Figs. 3d and 3e. The derivatives of the temperature difference were calculated using central difference approximations. The rate of change in the temperature difference, Fig. 3d, reaches a peak value of +0.4 K/s at $t = 18$ s. The second time derivative of the temperature difference, $d^2(\Delta T)/dt^2$, is shown in Fig. 3e. The first peak in the transient occurs at $t = 13$ s and has a value of +0.13 K/s^2. The transient has a value of zero at the $t = 18$ s corresponding to the peak rate of change in the temperature difference and then reaches a second peak of −0.09 K/s^2 at $t = 19$ s. Note that the $d^2(\Delta T)/dt^2$ transient consists of an positive impulselike response followed by a exponentially decaying negative steplike response. During a sunset eclipse transition, the signs of the impulse and decaying step are reversed. Note that the $d^2(\Delta T)/dt^2$ transient has the same form as the thermal snap time history described earlier.

Satellite Dynamics Response

The equations of motion, Eq. (8), were numerically integrated using the central differences method to determine a solution for the dynamic response of the system. The simulation utilized five flexible modes, with a timestep based on the highest mode included. The rigid hub has a mass of 5000 kg and a radius of 1.0 m, whereas the solar panel has a length of 9 m and a width of 3 m. Additionally, the solar panel has a mass per unit length, ρA, of 7.4 kg/m and a bending stiffness EI of 2.0E+04 N · m^2.

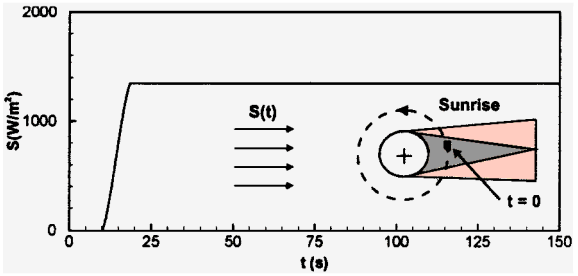

a) Solar heating history

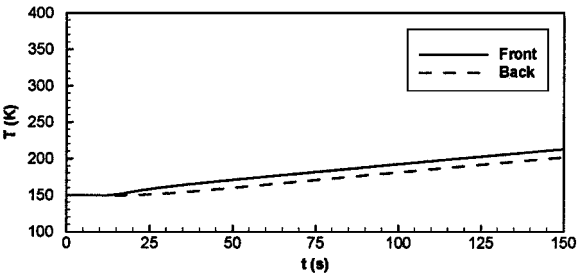

b) Surface temperatures

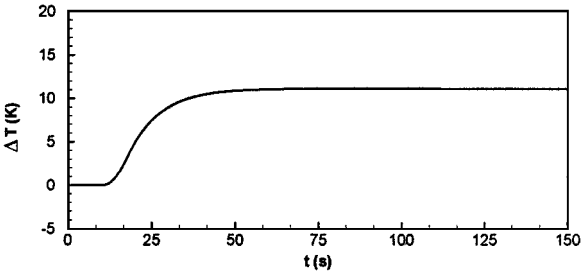

c) Through-the-thickness temperature difference

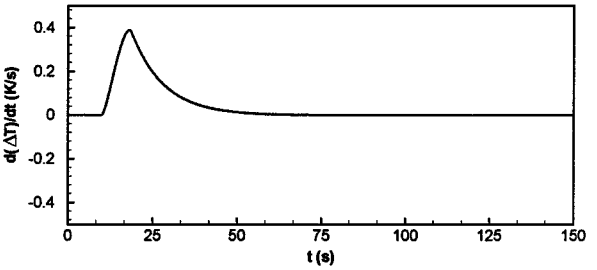

d) First time derivative of temperature difference

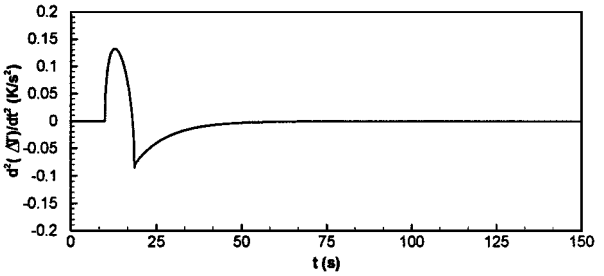

e) Second time derivative of temperature difference

Fig. 3 Solar panel thermal response during orbital sunrise.

The solar panel thermal-structural response is given in Figs. 4a–4d. The temperature difference through the thickness of the solar panel, Fig. 4a has a steady state value of 11 K with a rise time of approximately 75 s. Figure 4b presents a plot of the tip displacement $v(L, t)$ in the body fixed reference frame as a function of time. The tip displacement has a steady state value of -0.4 m with negligible superimposed oscillations. The maximum peak-to-peak amplitude of the oscillations (solar panel jitter) is less than $5.0E-05$ m and is too small to be seen in the figure. Thus, the solar panel motions may be classified as a quasi-static response. The solar panel exhibits velocity and acceleration transients of approximately 100-s duration that are initiated as the satellite enters the penumbra. The duration of the transients corresponds closely to the rise time for the temperature difference response. The tip velocity, Fig. 4c, has a peak value of -0.026 m/s that occurs at $t = 18$ s, corresponding to the time at which the temperature difference reaches its maximum rate of change (see Fig. 3). The acceleration at the free end of the solar panel, Fig. 4d, exhibits a characteristic thermal snap history with the addition of a small superimposed 0.5 Hz component corresponding to the fundamental frequency of the coupled system. The values of the first and second peaks of the acceleration transient are -0.0061 and $+0.0032$ m/s^2, respectively. Note that even though vibrations are negligible in the displacement response, their presence is still manifested in the accelerations.

The rigid hub response is presented in Figs. 4e–4h. The solar panel motions result in an internal disturbance torque that acts to change to orientation of the hub. The thermally induced disturbance torque $T_{\mathrm{TID}}(t)$, shown in Fig. 4e, displays a characteristic thermal snap profile. The disturbance torque has overall peak values of $+1.1/-0.6$ N · m with small amplitude damped oscillations at a frequency of 0.5 Hz due to the low level appendage dynamics. The disturbance torque is dominated by the quasi-static term whose form is determined by the second time derivative of the temperature difference. However, due to the presence of the vibratory terms, Eq. (9) predicts values for the first and second peaks in the torque that are, respectively, 30 and 15% greater than if only the quasi-static terms were considered. Thus, it is important to include both quasi-static and dynamic terms when calculating thermally induced disturbance torques. The attitude angle θ response, Fig. 4f, consists of a slowly developing rotation in the direction opposite of the solar panel motions. The attitude angle has a steady state value of 0.01 rad with negligible jitter (attitude angle jitter $< 1E-05$ rad). The attitude response exhibits rate and acceleration transients similar to the solar panel response, but with the signs reversed because the hub motions are always opposite those of the solar panel. The attitude rate, Fig. 4g, has a peak value of $9.1E-04$ rad/s that occurs at the same time as the peak in the solar panel velocities. The attitude acceleration, Fig. 4h, exhibits the characteristic thermal snap history with peak values of $+2.2E-04$ and $-1.2E-04$ rad/s^2.

Recall from the satellite dynamics analysis that for a quasi-static response, the solar panel accelerations and the corresponding disturbance torque acting on the rigid hub are directly proportional to the second time derivative of the temperature difference, $\mathrm{d}^2(\Delta T)/\mathrm{d}t^2$. Thus, thermal snap disturbances are characterized by the form of the $\mathrm{d}^2(\Delta T)/\mathrm{d}t^2$ transients that consist of an impulselike response followed by a exponentially decaying steplike response of the opposite sign. In contrast to the thermal snap disturbances illustrated here, a thermally induced vibrations disturbance transient exhibits oscillatory behavior and is larger in magnitude and longer in duration due to large amplitude solar panel vibrations.

Although considerable attention has been focused on the analysis of satellite disturbance data and analytical modeling of these phenomena, relatively few experimental studies have examined the thermal-structural behavior of satellite appendages. In the following section, the details of an experimental investigation performed to study solar panel thermal-structural behavior in the laboratory are presented.

Experimental Study

For the experimental study, the objectives were to investigate the behavior of solar panel flight hardware and to provide data for validation of finite element models. The following sections describe the laboratory test setup for the solar panel experiments and representative test results demonstrating key aspects of the thermal-structural behavior.

Test Setup

The laboratory experiments subject a solar panel test article to radiant heating on one face and measure the resulting thermal and structural responses. A photograph of the test setup for the solar

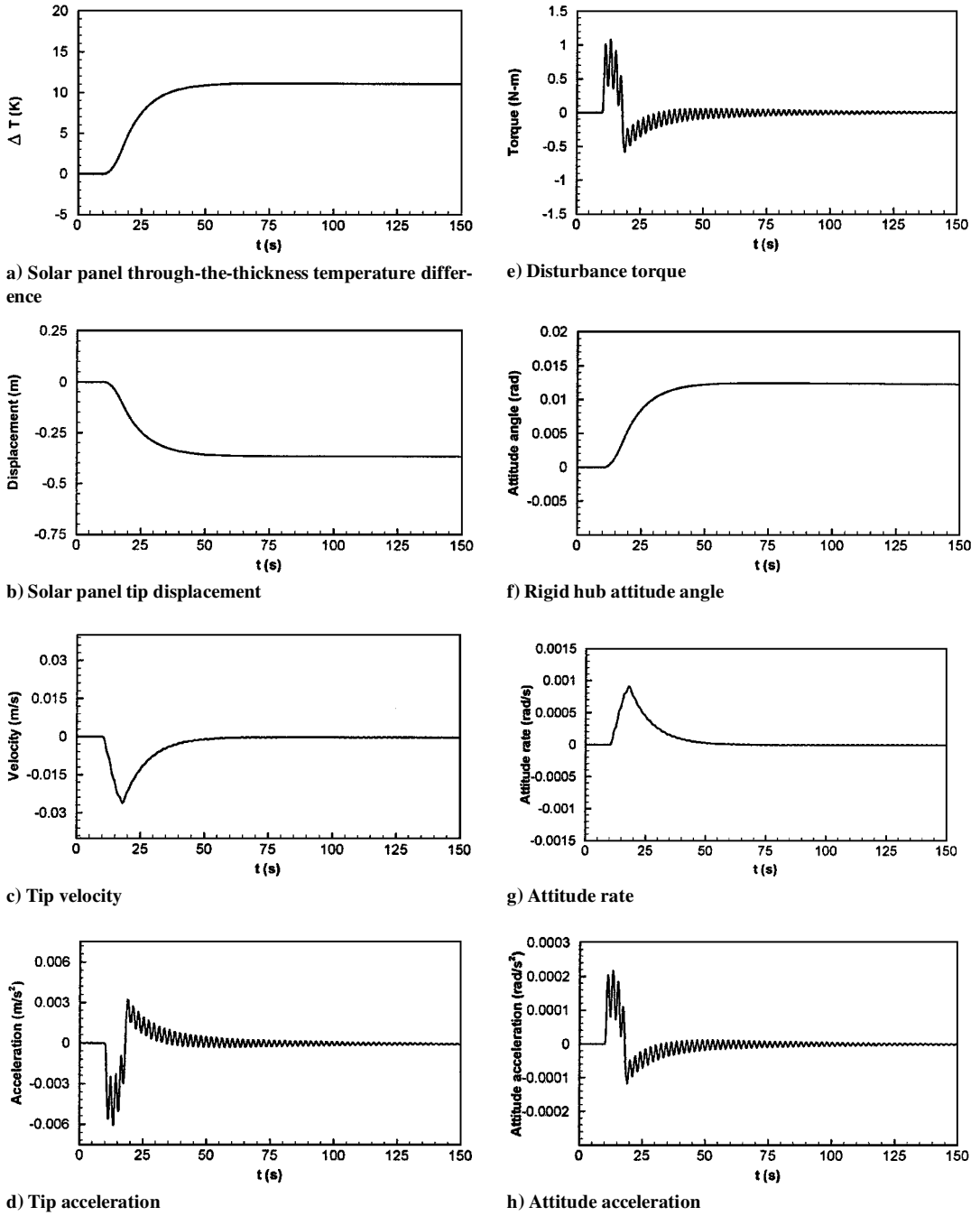

Fig. 4 Dynamic response of simple satellite during sunrise eclipse transition.

panel experiments is presented in Fig. 5a. The test setup consists of the following elements: a backstop support structure to which the solar panel is mounted, an array of infrared lamps for heating the panel, the TRACE solar panel test article, and instrumentation for recording the thermal-structural response. The backstop is constructed of structural steel I-beams mounted directly to the wall of the laboratory and acts as a rigid support structure. The solar panel is attached via a mounting plate that serves as an interface between the solar panel deployment hinges and the backstop. Radiant heating is provided by an array of quartz tube/tungsten filament infrared lamps that are capable of heating an area approximately 1300×800 mm. The lamp array is located at a fixed stand-off distance of 400 mm from the undeformed solar panel and is mounted such that the heat flux is directed normal to the surface of the panel. Heat flux characterization tests are performed to determine the spatial and temporal characteristics of the heat flux produced by the lamp array. For the tests reported, the lamp array provided an incident heat flux of 2000 W/m^2 on the front surface of the solar panel. The TRACE solar panel has an overall size of 960×510 mm and utilizes a metallic sandwich panel construction consisting of 0.254 mm thick aluminum 6061-T6 facesheets adhesively bonded to a 9.5-mm thick aluminum 5056-H39 honeycomb core. Machined aluminum structural inserts are placed throughout the substrate for the purpose of mounting components to the solar panel. The surfaces of the solar panel are painted with high-temperature paint to provide known surface properties. The heated side of the panel is painted flat black ($\alpha = 0.9$, $\varepsilon = 0.9$), whereas the unheated side is painted white ($\varepsilon = 0.9$). The test setup uses the same design deployment hinges to attach the solar panel to the mounting plate as are used to attach the actual solar panels to the satellite bus. To isolate the effects of the solar panel from that of the deployment hinge mechanisms, an alternate pair of structural supports was fabricated. The alternate supports, referred to henceforth as the rigid supports, consist of a pair of machined solid steel blocks of approximately the same overall size as the deployment hinges.

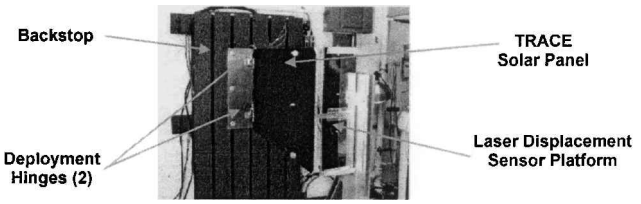

a) Photograph of test setup

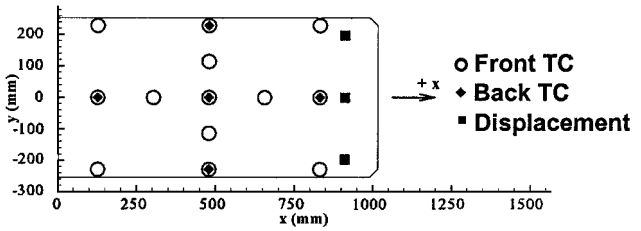

b) Schematic of solar panel showing coordinate system and measurement locations

Fig. 5 TRACE solar panel thermal-structural experiments.

The solar panel experiments characterize both the transient and steady-state response of the test article in terms of front (heated) and back (unheated) surface temperatures, through-the-thickness temperature differences, and displacements at the free end of the panel. Measurement locations on the solar panel are shown schematically in Fig. 5b. Thermocouples (Type T, 30 gauge) are used to measure the temperature at 13 points on the heated surface and five points on the unheated surface and to provide measurements of the through-the-thickness temperature differences at five points. Displacements at the free end of the solar panel are measured using laser displacement sensors. These sensors provide noncontact measurement of the displacements with a resolution of 0.01 mm. Three sensors measure displacements at a fixed distance of 910 mm from the supported end of the panel at heights corresponding to the top edge ($y = 200$ mm), centerline ($y = 0$ mm), and bottom edge ($y = -200$ mm) of the panel. During postprocessing of the test results, the velocity and acceleration of the solar panel are calculated from the displacement data using finite difference approximations.

For a typical test, a run begins when the data acquisition system is activated and 20 s of data are obtained with the test article at room temperature. Then, the infrared lamp array is turned on, providing a rapid heating profile that simulates a sunrise eclipse transition. The lamp array is operated at a constant power level for a duration of 2000 s, at which time the solar panel has reached thermal equilibrium. Next, the infrared lamp array is turned off, simulating the rapid decrease in heating that occurs as a satellite crosses into orbital eclipse.

Test Results

Results are now presented to demonstrate the thermal-structural response of the TRACE solar panel for the case of deployment hinge supports. Figure 6 presents results for the incident heat flux, through-the-thickness temperature difference, displacement, velocity, and acceleration of the solar panel for the first 100 s of a typical test run. The incident heat flux at the geometric center of the solar panel is shown in Fig. 6a. The heat-up transient consists of two parts: a rapid rise in the heat flux lasting approximately 10 s followed by a more gradual rise to steady-state lasting approximately another 200 s. The first phase corresponds to the initial rapid rise in the infrared lamp filament temperatures, whereas the second phase relates to the slower response time of the quartz tube envelopes. This heating history is satisfactory for simulating orbital eclipse transition heating because it approximates the rapid change in solar heating (lasting approximately 10 s for low Earth orbit satellites) that occurs as a satellite passes through the penumbra. The temperature difference at the geometric center of the panel, Fig 6b, rises rapidly following the initiation of rapid heating from the lamp array at $t = 20$ s, and reaches a steady-state value of 9 K approximately 200 s later. The rise time for the solar panel temperature difference is greater in the laboratory than in space because the infrared lamp array takes longer to transition from zero to full heating.

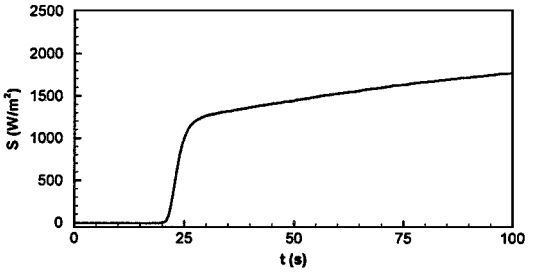

a) Incident heat flux

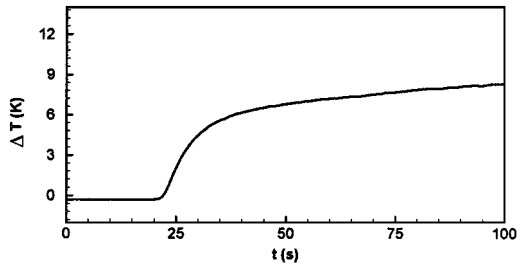

b) Through-the-thickness temperature difference

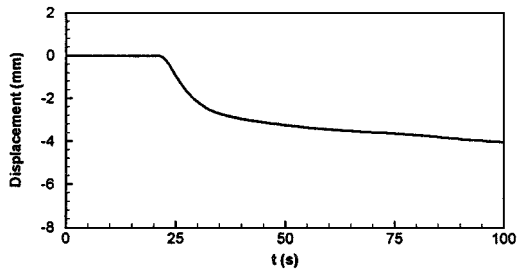

c) Displacement at free end

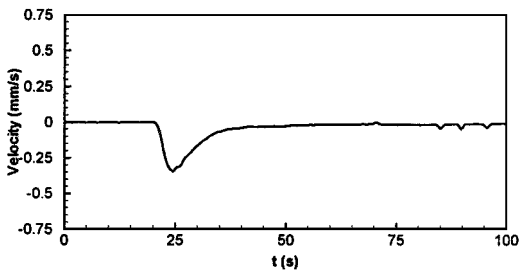

d) Calculated velocity

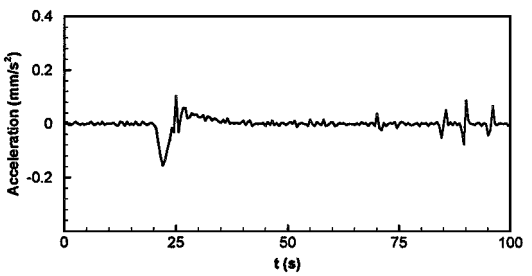

e) Calculated acceleration

Fig. 6 Representative laboratory test results for TRACE solar panel.

The temperature difference through the thickness of the panel results in a time-varying thermal moment that causes the panel to bend away from the direction of the applied heating. The displacement at the free end of the solar panel ($x = 910$ mm, $y = 0$ mm), Fig. 6c, reaches a steady state value of -5 mm in approximately 200 s. The displacements at the top and bottom edges of the solar panel are approximately 10% greater than that measured

along the centerline, which is indicative of thermal bending of the panel about its centerline (x axis). The displacements develop on the same time scale as the temperature difference, and the response is a quasi-static TISM. Recall that even though the displacements are classified as quasi-static, rapid structural motions during heat-up result in acceleration transients that impart disturbance torques on satellites. Figures 6d and 6e present plots of the calculated velocity and acceleration at the free end of the solar panel. During heat-up, there is a velocity transient (Fig. 6d) as the solar panel moves away from the heat source. The transient consists of a rapid change from the initial zero velocity state to a maximum value of -0.32 mm/s. The acceleration transient (Fig. 6e) consists of two parts. The first part involves an impulselike response followed by a zero crossing at the time corresponding to the maximum velocity. The second part of the transient consists of another peak that has the opposite sign of the first peak followed by a decaying exponential response to zero. The first and second peak values of the heat-up acceleration transient are -0.15 and 0.03 mm/s^2. Note that the acceleration transient observed in the solar panel laboratory experiments has the same form as the solar panel acceleration transient predicted by the analytical solution. Thus, the acceleration transients observed in the experiments are representative of the thermal snap disturbances known to affect satellites with rigid panel solar arrays.

In addition to the thermal snap acceleration transient during heat-up, several intermediate acceleration transients are observed after approximately 75 s of heating. Reference 2 presents the details of a study completed to investigate the source of the intermediate disturbances. These disturbances were suspected to be related to the solar panel deployment hinges. A series of tests were completed in which the deployment hinges were replaced by rigid steel blocks to eliminate the nonlinearities associated with free-play and hysteresis in the hinge mechanisms. Figure 7 presents a comparison of the heat-up acceleration histories for the deployment hinge and the rigid support cases. The intermediate transients are consistently absent from the response of the rigidly supported system, thereby identifying the hinges as the source of the intermediate disturbances. The intermediate transients are believed to be thermal creak disturbances resulting from thermally induced stick-slip motions within frictional interfaces in the hinge mechanisms.

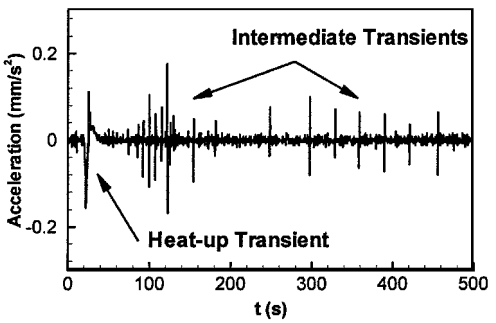

a) Deployment hinge supports

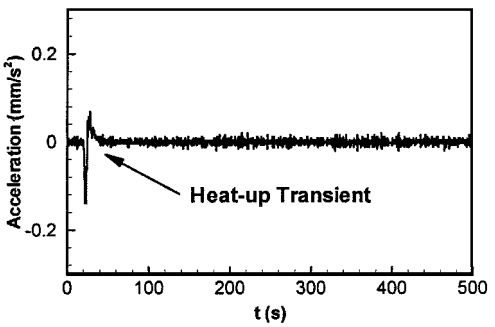

b) Rigid supports

Fig. 7 Comparison of solar panel acceleration histories.

Analysis of Experiments

The objective of this analysis is to predict the thermal-structural behavior of the TRACE solar panel observed in the laboratory experiments. Recall that a one-dimensional thermal analysis and a beam structural model were presented earlier for studying the thermal-structural response of simplified solar panels in the space environment. Since thermal loading in the laboratory differs substantially from the space environment, it is necessary for this thermal analysis to model effects such as nonuniform radiant heating and natural convection to account for in-plane as well as through-the-thickness temperature variations. Additionally, the laboratory experiments demonstrated that the solar panel structural response exhibits plate behavior involving thermal bending deformations about two axes. Modeling these effects necessitates the use of a three-dimensional finite element model to represent the laboratory test environment and the thermal-structural behavior of the test article accurately.

The finite element program ABAQUS[12] was used to perform the thermal and structural analyses. The elements selected to model the solar panel are general purpose, first order shell elements with four nodes (ABAQUS DS4 elements for the thermal model and S4R elements for the structural model) and allow for through-the-thickness temperature variations. The elements account for the sandwich construction of the solar panels with three layers corresponding to the top facesheet, core, and bottom facesheet. The honeycomb core was modeled using effective thermal and structural properties. Additionally, the model includes approximate representations of the structural inserts. The finite element mesh consisted of 21 elements along the length of the panel and 8 elements across the width of the panel. The same mesh and number of temperatures through the thickness were used in the thermal and structural models.

The transient thermal-structural response of the solar panel was predicted utilizing a sequentially coupled thermal stress analysis in which the nodal temperature histories from an uncoupled thermal analysis serve as the thermal loading in a static structural analysis. The uncoupled thermal analysis calculates the transient response of the solar panel subject to a spatially nonuniform, time-varying heat flux on its front surface with energy loss from natural convection and thermal radiation on both front and back surfaces. The temporal and spatial characteristics of the incident heat flux are determined from independent laboratory tests and are included in the analysis by specifying a time-varying amplitude for the incident flux and mapping the appropriate spatial variation of the heat flux over the finite element mesh. The sequentially coupled structural analysis then computes the quasi-static response of the solar panel to the specified time-varying temperatures from the thermal analysis. The case of the rigid structural supports was chosen for the comparison of analysis and experiment because modeling the complex nonlinear behavior of the deployment hinges is beyond the scope of this study. Thus, in the structural model, the solar panel is free along three edges and fixed against rotation and displacement along a portion of its fourth edge corresponding to the location of the supports. The structural finite element model was validated by performing a frequency analysis of the solar panel, whose mass properties are well known, and comparing the predicted value for the fundamental frequency with the value measured in the laboratory. The finite element model correctly predicts the fundamental frequency for the solar panel with an error of less than 3%.

A detailed comparison of test results and predictions from the finite element model for the thermal-structural response of the solar panel is given in Ref. 2. Figure 8 presents a comparison of analytical and experimental results for the structural response. Figure 8a presents a plot of the predicted and measured displacements at the free end ($x = 910$ mm and $y = 0$ mm) of the solar panel vs time for the first 100 s of the test run. The finite element analysis predicts the general trend in the displacement history correctly; however, the predicted values are greater than the test results. Steady-state values for the displacement from the finite element analysis and the experiment are -6.5 and -5.7 mm respectively. The difference between the measured and predicted steady-state displacements is 8%. Figure 8b presents a plot of the velocity during the heat-up

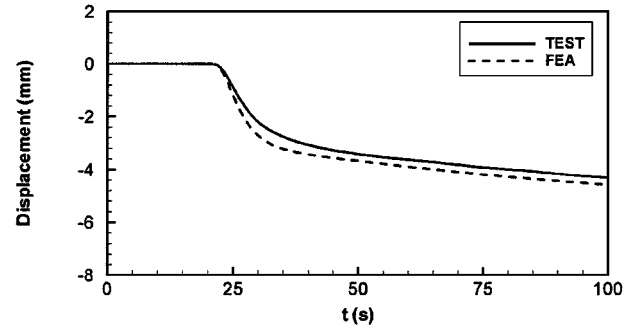

a) Displacement

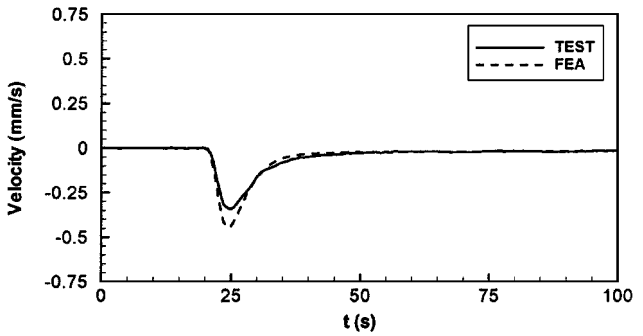

b) Velocity

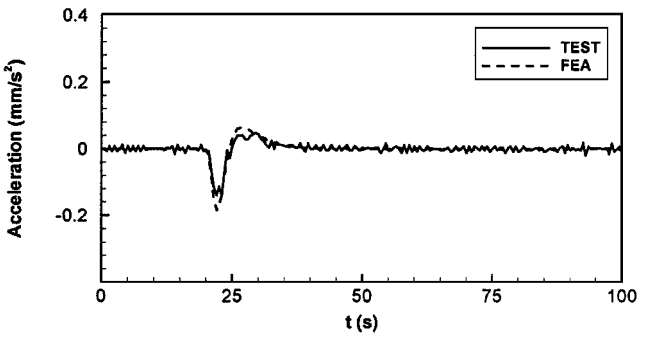

c) Acceleration

Fig. 8 Comparison of predictions from finite element analysis and test results for solar panel structural response to simulated orbital eclipse transition heating.

transient. The peak values in the velocity transient from the finite element analysis and the experiment are −0.50 and −0.44 mm/s, respectively. The finite element model predicts the form of the transient correctly; however, the predicted peak velocity is greater than the measured response by 14%. The discrepancy between the predicted and measured values for the velocity transient peaks results from the overprediction of the solar panel displacements. A plot of the acceleration transient during heat-up is presented in Fig. 8c. The predicted and measured values for the first peak in the acceleration transient are −0.18 and −0.14 mm/s^2, corresponding to a 28% difference. The finite element model correctly predicts the form of the acceleration transient that has the characteristic thermal snap response. However, as was the case with the velocity transients, the acceleration values predicted by the analyses are greater than the test values.

The analysis of the laboratory experiments demonstrates that a three-dimensional finite element model is required to model solar panel thermal-structural behavior accurately in the presence of nonuniform heating and natural convection. Qualitatively, it was found that the finite element models predict the thermal-structural behavior observed in the laboratory experiments correctly. Importantly, the finite element models are able to predict the thermal snap disturbance transients observed in the experimental studies. Quantitatively, the predictions for the response of the TRACE solar panel show fair agreement with test results. The discrepancies between the predicted and observed behavior are due to a combination of difficulties in modeling the laboratory thermal environment, the solar panel construction, and the structural supports.

Conclusions

This paper has presented analytical and experimental investigations of solar panel thermal snap disturbances. The following insights were gained from the thermally induced satellite dynamics analysis and the solar panel thermal-structural experiments:

1) The critical parameters from the thermal response of rigid panel solar arrays (solar panels) are the through-the-thickness temperature difference and its time derivatives. Sudden changes in solar panel thermal loading, such as during orbital eclipse transitions or steplike changes in heating from the infrared lamp array in the laboratory tests, result in the rapid development or decay of temperature differences and cause short duration transients in the histories of the first and second time derivatives of the temperature difference.

2) The solar panel structural response is driven by the time-varying through-the-thickness temperature differences and may consist of either quasi-static or thermally induced vibrations motions. Solar panels undergoing quasi-static deformations experience brief thermal snap acceleration transients during heat-up and cool-down, whereas solar panels experiencing thermally induced vibrations exhibit acceleration histories involving decaying oscillations.

3) Rapid structural motions during heat-up and cool-down result in acceleration transients that impart a disturbance torque to the main body of a satellite. The disturbance torque is directly proportional to the solar panel accelerations; thus, the time history of the torque has the same form as that of the accelerations. Thermally induced disturbance torques from thermal snap disturbances are dominated by solar panel accelerations resulting from $d^2(\Delta T)/dt^2$ transients, whereas torques from thermally induced vibrations disturbances are dominated by solar panel accelerations resulting from vibrations of the system.

Finally, comparison of the attitude disturbances observed in flight data from the UARS satellite and the disturbance transients predicted by the satellite dynamics analysis and observed in the laboratory experiments reveals the same characteristic thermal snap profile in each case. Although this research has provided significant insight into solar panel thermal snap, ultimately the phenomena should be the focus of a space-based experimental study. This research is necessary to overcome the limitations of ground-based testing of space structures and to provide in situ measurements of TISMs for validation of analytical models.

Acknowledgments

Support for this research was provided by the NASA Graduate Student Researchers Program and the Virginia Space Grant Consortium. The authors would like to acknowledge our technical advisors Brantley Hanks, Mark Lake, and Marvin Rhodes from NASA Langley Research Center. Additionally, the authors wish to thank Mike Adams and Darrell Zimbelman from NASA Goddard Space Flight Center for their support of the TRACE solar panel experiments.

References

[1] Thornton, E. A., *Thermal Structures for Aerospace Applications*, AIAA Education Series, AIAA, Reston, VA, 1996, pp. 343–354.

[2] Johnston, J. D., "Thermally-Induced Structural Motions of Satellite Solar Arrays," Ph.D. Dissertation, Dept. of Mechanical and Aerospace Engineering, Univ. of Virginia, Charlottesville, VA, May 1999.

[3] Foster, R. S., "Thermally-Induced Vibrations of Spacecraft Booms," Ph.D. Dissertation, Dept. of Mechanical and Aerospace Engineering, Univ. of Virginia, Charlottesville, VA, May 1998.

[4] Kim, Y. A., and McManus, H. L., "Thermally-Induced Vibrations of Space Structures," *Thermal Stresses 97: Proceedings of the Second International Symposium on Thermal Stresses and Related Topics*, Lastran Corp., Honeoye Falls, NY, 1997, pp. 661–664.

[5] Bainum, P. M., Hamsath, N., and Krishna, R., "The Dynamics and Control of Large Space Structures After the Onset of Thermal Shock," *Acta*

Astronautica, Vol. 19, No. 1, 1980, pp. 1–8.

[6]Zimbelman, D. F., "Thermal Shock and Its Effect on Spacecraft Attitude Control," Ph.D. Dissertation, Dept. of Aerospace Engineering Sciences, Univ. of Colorado, Boulder, CO, Aug. 1990.

[7]Zimbelman, D. F., Dennehy, C. J., Welch, R. V., and Born, G. H., "A Technique for Optimal Temperature Estimation for Modeling Sunrise/Sunset Thermal Snap Disturbance," *Journal of Spacecraft and Rockets*, Vol. 28, No. 4, 1991, pp. 448–456.

[8]Johnston, J. D., and Thornton, E. A., "Thermally-Induced Attitude Dynamics of a Spacecraft with a Flexible Appendage," *Journal of Guidance, Control, and Dynamics*, Vol. 21, No. 4, 1998, pp. 581–587.

[9]Johnston, J. D., and Thornton, E. A., "Thermal Snap of Satellite Solar Panels," *Proceedings of the 1999 Flight Mechanics Symposium*, NASA Goddard Space Flight Center, NASA CP 209235, 1999, pp. 215–229.

[10]Lambertson, M., Underwood, S., Woodruff, C., and Garber, A., "Upper Atmosphere Research Satellite Attitude Disturbances During Shadow Entry and Exit," American Astronautical Society Paper 93-319, 1993.

[11]Baker, R. M. L., *Astrodynamics: Applications and Advanced Topics*, Academic, New York, 1967, pp. 191–194.

[12]*ABAQUS User's Manual*, ver. 5.7, Hibbett, Karlsson, and Sorenson, Pawtucket, RI, 1997.

[13]Junkins, J. L., and Kim, Y., *Introduction to Dynamics and Control of Flexible Structures*, AIAA Education Series, AIAA, Washington, DC, 1993, pp. 139–225.

M. P. Nemeth
Associate Editor